

Direct Measurement of Nonresonant Multiphoton Ionization Profile for Xe Atoms* - dependence on incident laser wavelength and ionized charge state -

S. Ichimura

Ultra-fine Profiling Technology Research Laboratory, AIST, Tsukuba Central 2, 1-1-1 Umezono, Tsukuba 305-8568, Japan
s.ichimura@aist.go.jp

Received 27 January 2003; Accepted 1 February 2003

A method called nonresonant multiphoton ionization (NRMPI) gives high possibility of detecting "one atom/molecule" in gas phase, so that it has been widely used as a powerful tool for sputtered neutral mass spectrometry [1] and pressure measurement in extremely high vacuum region (lower than 10^{-9} Pa)[2]. It is well known that the possibility (P) of NRMPI strongly depends on incident laser power density (I) and, at relatively low power density condition, it shows the dependency of

$$P \propto I^n \quad (1)$$

where n is the number of photons necessary for ionization of a target atom/molecule[3]. Ionization probability comes to saturate at high power density condition.

When a laser beam is focused to target atoms/molecules with a conventional spherical lens, the beam diameter is minimum at a focal point of the spherical lens. Thus the laser power density is maximum at the focal point, and the probability of NRMPI of target atoms/molecules is maximum at the point. The far the distance from the focal point is, the lower the ionization probability is. Based on this simple consideration, it is deduced that the region of NRMPI has a spindle shape with its center at a focal point, as is schematically shown in Fig. 1.

Ichimura et al. has succeeded to confirm the spindle shape of the laser ionization region[4]. They ionized hydrogen molecules (ionization potential; 15.4 eV) with second harmonics of a pico-second YAG laser (wavelength: 532 nm, photon energy 2.33 eV). A special imaging detector consisted of a static lens (with

magnification of 16), a microchannel plate (MCP) detector, and a CCD camera, etc.[5], was used for the experiment. Ions generated in the ionization region were projected onto the MCP detector, thus a flat spindle image was observed on it. From the size of the flat spindle image and the magnification of the static lens system, they have estimated a volume of the ionization region and showed the evidence of "one atom/molecule" detection with high accuracy[6].

The ionization of hydrogen molecules with second harmonics of a YAG laser is 7-photon process, so it is natural that the ionization probability rapidly decreased around the focal point, leading to a spindle shape of the ionization region. However, the probability of NRMPI in area a little far from the focal point may remain at a certain level if an atom/molecule with low ionization potential is ionized by a laser beam with high photon energy. Since observed profile of NRMPI is determined by multiplication of laser beam size and ionization probability, other shapes than a spindle shape may be observed in such a case.

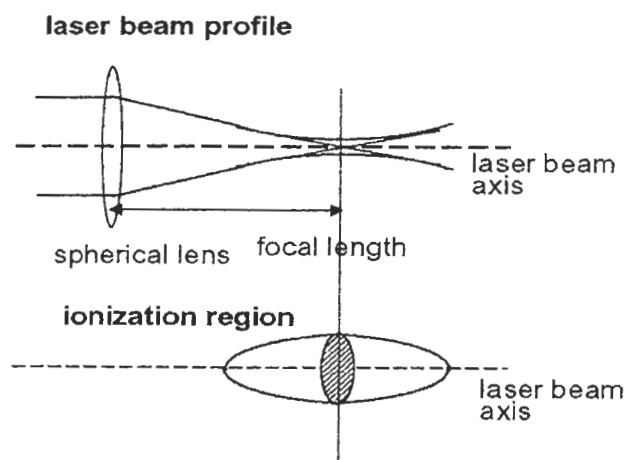


Fig.1. Scheme of a laser beam profile near a focal point of a spherical lens, and estimated shape of the ionization region near the focal point

* Dedicated to the late Dr. Tetsu Sekine. It is one of my best memories that the first work of the direct observation of the ionization region was presented at AVS international meeting in front of Sekine-san, and he gave me valuable suggestion after the presentation.

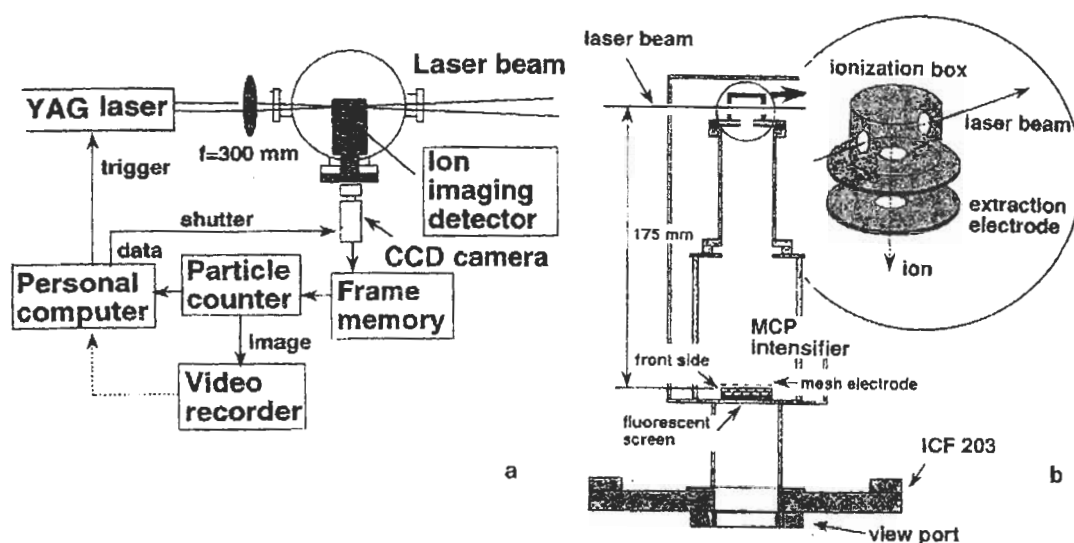


Fig.2. (a) Scheme of the experimental setup for the direct observation of the region of NRMPI, and (b) enlarged scheme of ion imaging detector.

The aim of the present report is to show experimental results that give other shape of the ionization region than the spindle shape mentioned above. It is also aimed to explain the method to estimate the shape of the ionization region, since the information of the ionization region is valuable for the estimation of useful yield in SNMS as well as for absolute pressure measurement by laser ionization. Choosing Xe atoms as target for NRMPI, the profile corresponding to various ionized state (Xe^+ , Xe^{2+} , and Xe^{3+}) was measured under incidence of laser beam with various laser wavelength, *i.e.*, 2nd (2ω) and 3rd (3ω), and 4th (4ω) harmonics of YAG laser output (fundamental wavelength ω ; $1.06 \mu\text{m}$). Depending on the combination of ionization condition and incident laser wavelength, the ionization region showed two types of shape (either spindle shape or bow tie shape) in the present experiment as shown below.

Figure 2(a) shows experimental setup schematically. A laser beam from a pico-second YAG laser was focused into a vacuum chamber where Xe gas was filled at a pressure of 5×10^{-6} Pa. The wavelength of the incident laser beam was chosen from one of the higher harmonics (2ω , 3ω , 4ω) of the YAG laser, while the incident laser intensity was kept always at 10 mJ/pulse. The laser beam was focused with a spherical lens (focal length; 300 mm), so the focused power density was expected to reach 10^{13} W/cm² under the condition. Xe ions generated at the focal

point were projected on a MCP intensifier, and an image on the intensifier was taken with a CCD camera and recorded as video image for later processing.

Figure 2(b) shows enlarged scheme of the ion-imaging detector. A laser beam passes the detector through a hole (8 mm in diameter) of the top electrode with a hat shape, and generated ions are extracted out through a hole (8 mm in diameter) of the extraction electrode with disk shape. An enlarged image (magnification; 16) of the ionization region can be projected on the MCP intensifier when +300 V was supplied to the top electrode and -300 V was supplied to the extraction electrode.

The distance between the laser beam and the MCP intensifier was 175 mm. The distance is long enough to distinguish ionized species by time-of-flight (ToF) technique. Figure 3 shows an example of ToF spectrum obtained with the imaging detector. The spectrum was taken with 3ω of the YAG laser at Xe pressure of 5×10^{-6} Pa. Signals from different ionization state of Xe atom (Xe^+ , Xe^{2+} , and Xe^{3+}) are recognizable together with other signals originating from residual gas ionization such as H^+ , O^+ , H_2O^+ , etc. Thus it is possible to get the image of the ionization region corresponding to a selected ion species/ionization state if we can add a function of timing gate to the imaging detector. The function was given by placing in front of the MCP intensifier a mesh grid, to which +300V was always supplied except when the arrival time of the

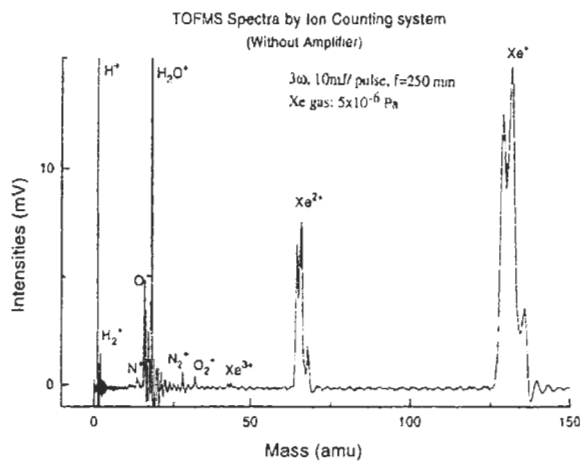


Fig.3. A time-of-flight (ToF) spectrum obtained with the imaging detector for the incidence of picosecond YAG laser (3rd harmonics, pulse power; 10 mJ) to Xe gas target maintained at a pressure of 5×10^{-6} Pa.

selected species/ionization state; only +100 V was supplied during the arrival time by supplying -200 V negative pulse to positive bias of +300 V.

Figure 4 shows the image of the ionization region for Xe^{3+} ions taken under the incidence of 3w of YAG laser. With the lens magnification and the effective size of the MCP intensifier (32 mm in diameter), the detector could take an image corresponding to a part (about 2 mm in length along the laser beam) of the ionization region. So, in usual case, the spherical lens position has to be shifted along the laser beam direction (X-direction) in order to take the whole area of the ionization region. 5 photographs in Fig. 4 were taken at different spherical lens positions of $X = 5$ to $X = 9$, with 1 mm step to the next lens position. Brightness change in each photograph represents the change of ionization probability along the laser beam path, which was experimentally obtained using the detector by counting the number of ions generated at any point of the image.

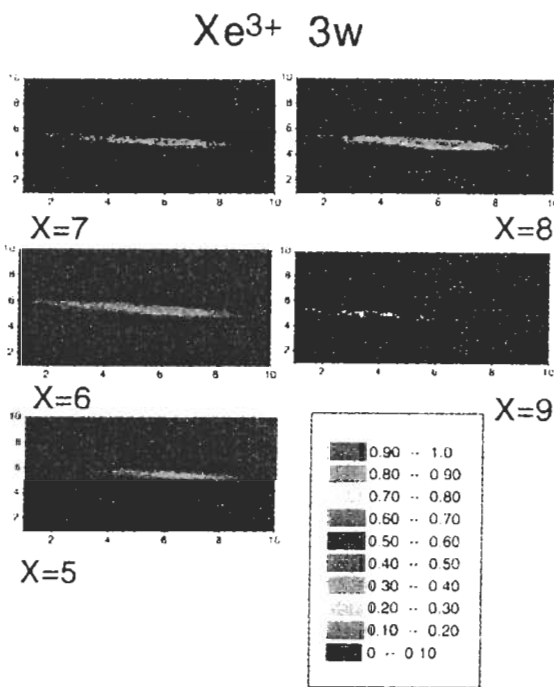


Fig.4. Images of the spatial distribution of Xe^{3+} ionization for the incidence of 3ω of YAG laser to Xe gas of 5×10^{-6} Pa. Each image was taken at different spherical lens position indicated by x value (in mm unit). Ionization probability of any point in the image is classified into 10, and is indicated with different brightness. The same probability scale is used for all images shown in Fig.4 and Fig.5.

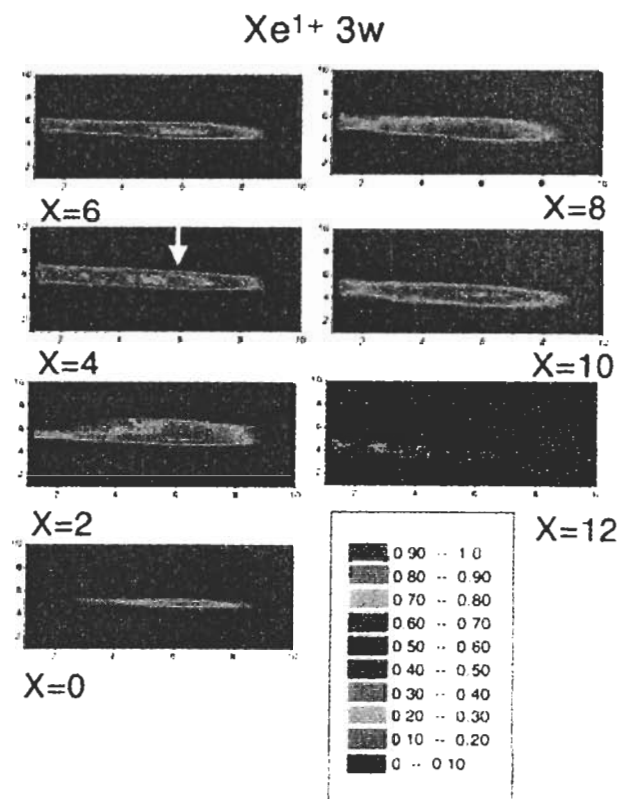


Fig.5. Images of the spatial distribution of Xe^{1+} ionization for the incidence of 3ω of YAG laser to Xe gas of 5×10^{-6} Pa. Each image was taken at different spherical lens position indicated by x value (in mm unit). Ionization probability of any point in the image is classified into 10, and is indicated with different brightness. The same probability scale is used for all images shown in Fig.4 and Fig.5.

The ionization probability was classified into 10 as shown in the bottom of Fig.4.

Since the ionization energy of Xe^{3+} ion is 32.1 eV while the photon energy of 3ω of YAG laser is 3.5 eV (wavelength; 355 nm), the ionization occurred by 10-photon process. Reflecting the large number of photons necessary for the ionization, the ionization region had a spindle shape like that of H_2 ionization with 2ω of YAG laser, which can be clearly seen in Fig. 4. It was also possible from Fig. 4 to conclude that the length of the observed ionization region was about 4 mm. The shape of the ionization region and its length were nearly same for the ionization of Xe^{2+} ions (ionization potential; 21.2 eV) with 3ω of YAG laser.

Figure 5 shows the image of the ionization region for Xe^+ ions taken under the incidence of 3ω of YAG laser. The spherical lens position was moved from $X = 0$ to $X = 12$ with 1 mm step in this case, and photographs taken at each lens position was shown in Fig. 5. Brightness in the photographs represents the probability of ionization, and the area corresponds to the brightness level of 0.90 - 1.0 (which is indicated with arrow in Fig. 5) means that the ionization probability is the highest at the area. It should be noted that the same probability scale was used both in Fig. 4 and Fig. 5.

Looking at the photographs in Fig.5 from bottom left to top left, it is easily noticed that the area of the ionization region became wide (at $X = 2$) then became narrow (at $X = 6$), while the area showing maximum ionization probability appeared in the photographs taken at $X = 4$ and 6. When we look at the photographs from top right to bottom right, it is also noticed that the area became wide again (at $X = 8$ and 10) and then became narrow. It is clear, therefore, that the ionization region had a bow tie shape in this case.

The ionization energy of Xe^+ ions was 12.1 eV, so that 4-photon process occurred in the ionization with 3ω of YAG laser. For the ionization of Xe^+ ions with 2ω of YAG laser (532 nm, 2.33 eV), which needs 6 photons, a spindle shape of the ionization region was observed instead of a bow tie shape. The ionization of Xe^{2+} with 3ω of YAG laser, which is 7-photon ionization process, showed a spindle shape as mentioned above. Therefore 5-photon process may be a critical point between the observation of spindle

shape and bow tie shape for the ionization of Xe under the incident laser power density of 10^{13} W/cm². We also tried to observe the image of the ionization area for Xe atoms with 4ω of YAG laser. However, the MCP intensifier had high sensitivity to such a laser with short wavelength (266 nm; 4.7 eV), and only white image in whole area was obtained. A MCP with gate function is necessary for the measurement, and is left for further study.

In summary, we could observe a laser ionization region having a bow tie shape for the first time. The bow tie shape of the ionization region appeared for the combination of lower ionization energy of target atom/molecule and larger photon energy of incident laser beam. In other cases, a spindle shape of the ionization region was observed. The experimental method to get the profile of ionization region is useful for SNMS and pressure measurement by laser ionization, especially in the determination of useful yield and in the determination of absolute density of atoms by the method.

ACKNOWLEDGEMENT

The author would like to express his sincere appreciation to Dr. H. S. Im for his help in the experiment of the present work. Thanks are also to Prof. T. Ikuta of the Osaka Electron-Communication Univ. for his contribution to data analysis.

References

- [1] for example; R. Jede, O. Ganschow, and U. Kaiser, *Practical Surface Analysis Vol.2, Ion and Neutral Spectroscopy*, p425, D. Briggs and M.P. Seah eds., Wiley, Chichester (1992).
- [2] K. Kokubun, S. Sekine, S. Ichimura, A. Kurokawa, and H. Shimizu, *Vacuum* **47**, 557 (1996).
- [3] for example; J. Morellec, D. Normand, and G. Petit, *Adv. At. Mol. Phys.* **18**, 97 (1982).
- [4] S. Ichimura, S. Sekine, K. Kokubun, and H. Shimizu, *J. Vac. Sci. Technol.* **A12**, 1734 (1994).
- [5] S. Ichimura, S. Sekine, H.J. Steffen, K. Kokubun, and H. Shimizu, *Jpn. J. Appl. Phys.* **33**, L135 (1994).
- [6] S. Ichimura, K. Kokubun, H. Shimizu, and S. Sekine, *Vacuum* **47**, 545 (1996).